BMC Medical Imaging

RESEARCH

Open Access

Comparative analysis of apparent diffusion coefficient (ADC) metrics for the differential diagnosis of breast mass lesions

Yangping Yang[1,2†], Jiong Liu[1,3†] and Jian Shu[1,3*]

Abstract

Background Breast cancer's diagnostic challenge is amplified by its heterogeneity. Diffusion-Weighted Imaging (DWI) offers promising avenues for precise tumor characterization through Apparent Diffusion Coefficient (ADC) metrics.

Purpose To investigate the diagnostic utility of advanced ADC metrics in distinguishing breast lesions using Magnetic Resonance Imaging (MRI).

Methods A retrospective cohort analysis of MRI data from 125 pathologically confirmed breast tumors was conducted. ADC values were independently measured by two physicians at the lesion sites and reference points (contralateral normal breast parenchyma, pectoralis major, and interventricular septum), from which advanced ADC metrics were calculated. Statistical analyses were applied to differentiate ADC metrics between malignant and benign groups. ROC curves assessed the diagnostic efficacy of individual ADC metrics. A binary logistic regression model incorporating ADC metrics and age was developed, with its diagnostic superiority evaluated through multidimensional comparisons.

Results Of the 125 lesions, 77 were malignant and 48 benign. Significant differences in ADC metrics were found between malignant and benign tumors. Diagnostic analysis showed minimum ADC value (ADC_min) as the most effective single indicator, while the combined model, including age and average ADC value (ADC_avg), outperformed individual ADC metrics, demonstrating superior diagnostic accuracy (area under the curve (AUC) = 0.964). The combined model nomogram also showed improved clinical utility and a significant increase in diagnostic performance.

Conclusions Advanced ADC metrics significantly enhance the diagnostic accuracy for differentiating between benign and malignant breast lesions. The development of a combined model further refines breast cancer diagnostics, supporting the advancement towards precision medicine.

Keywords Breast tumor, Magnetic resonance imaging, Apparent diffusion coefficient, Differential diagnosis

†Yangping Yang and Jiong Liu contributed equally to this work.

*Correspondence:
Jian Shu
shujiannc@163.com

[1]Department of Radiology, The Affiliated Hospital of Southwest Medical University, No 25 Taiping St, Jiangyang District, Luzhou, Sichuan, PR China
[2]Department of Radiology, Chongzhou People's Hospital, Chengdu, China
[3]Nuclear Medicine and Molecular Imaging Key Laboratory of Sichuan Province, No 25 Taiping St, Jiangyang District, Luzhou, Sichuan, PR China

Background

Breast cancer remains one of the leading causes of cancer incidence and mortality among women worldwide, with over 2 million new cases reported annually [1]. The early and accurate differentiation between benign and malignant breast tumors is critical for optimizing clinical management, minimizing unnecessary invasive procedures, and improving patient prognosis. Moreover, malignant breast tumors exhibit a range of pathological and molecular subtypes, each presenting distinct diagnostic and therapeutic challenges [2]. The inherent heterogeneity of these tumors further necessitates the advancement of diagnostic methods to accurately characterize and develop tailored treatment strategies. Conventional imaging techniques, including mammography and ultrasound, are widely employed for the initial characterization of breast lesions. However, these methods often have limitations in distinguishing between benign and malignant lesions, particularly in dense breast tissue or complex cystic-fixed masses [3]. In contrast, breast magnetic resonance imaging (MRI), particularly when combined with functional imaging techniques such as diffusion-weighted imaging (DWI), has emerged as an important tool for assessing tumor biology [4, 5].

DWI assesses the microscopic movement of water molecules within tissues, with the apparent diffusion coefficient (ADC) serving as a key quantitative metric derived from this technique [6]. This metric non-invasively reflects the cellular density and membrane integrity of tumor tissue, thus assisting in the differentiation of benign and malignant breast lesions [7]. However, traditional focus on the mean ADC value (ADC_avg) may oversimplify the complex heterogeneity of breast tumors, and existing studies and meta-analyses often yield contradictory results. For instance, one meta-analysis suggests that lower ADC values are associated with higher Ki-67 expression [8], whereas another meta-analysis indicates that ADC cannot serve as a surrogate marker for Ki-67 expression in breast cancer [9]. Moreover, ADC values may be closely related to tumor cell density as well as the extracellular matrix (ECM) content [10], further complicating the use of ADC in breast cancer diagnosis. Thus, the mean ADC value alone may not adequately capture the diversity and biological characteristics of breast lesions.

In recent years, additional ADC-derived metrics, such as the minimum ADC value (ADC_min), relative minimum ADC ratio (rADC_min), and ADC coefficient of variation (ADC_cv), have been proposed. These metrics provide a more sensitive reflection of the diffusion characteristics within tumors, particularly in regions exhibiting significant heterogeneity. For example, ADC_min is better able to capture areas within tumors that are characterized by high cell density and restricted diffusion [11], while rADC, as a relative value, standardizes the lesion's ADC against normal tissue, thereby minimizing bias from interindividual tissue variability and improving diagnostic stability and accuracy [12]. Although these advanced ADC metrics demonstrate potential for enhancing the sensitivity and specificity of tumor diagnosis, most existing studies have evaluated these metrics in isolation, lacking comprehensive comparisons and discussions on their combined application.

Therefore, the aim of this study is to retrospectively analyze MRI data of pathologically confirmed breast tumors and systematically assess the diagnostic value of various derived ADC metrics in the differentiation of benign and malignant breast tumors. Furthermore, by constructing a combined predictive model, we seek to further improve the diagnostic accuracy for breast tumors, thereby offering novel approaches for early screening and precision treatment in clinical practice.

Methods

Patients

This retrospective study included pathologically confirmed breast tumor cases from a major medical center in Southwest China, recorded between January 2019 and June 2022. Patients were selected based on the following inclusion criteria: (1) breast tumors diagnosed via preoperative MRI; (2) all lesions on MRI were characterized by mass-like enhancement; (3) definitive pathological diagnosis. The exclusion criteria were as follows: (1) patients who underwent chemotherapy, biopsy, surgery, or other interventions before MRI; (2) incomplete clinical or imaging data; (3) patients with coexisting other malignant tumors; (4) lesions that were too small to delineate and obtain differential results (Fig. 1). Ethical approval was granted by the hospital's medical ethics committee, and informed consent was waived (Approval No. 2021[5]).

MRI protocol

MRI scans were performed using a Philips (Amsterdam, Netherlands) Ingenia 1.5 T superconducting scanner equipped with a dedicated breast coil. Patients were positioned prone to allow natural positioning of the breasts within the coil. The scanning protocol included T1-weighted imaging (T1WI), T2-weighted imaging with spectral attenuated inversion recovery (T2WI-SPAIR), DWI, and dynamic contrast-enhanced T1WI (DCE-T1WI). Specific scanning parameters for each sequence are outlined (Table 1). Gadopentetate dimeglumine was used as the contrast agent for DCE-T1WI.

Image processing and data measurement

Routine MR scanning, DWI imaging, and multi-phase dynamic enhancement scanning were performed on all

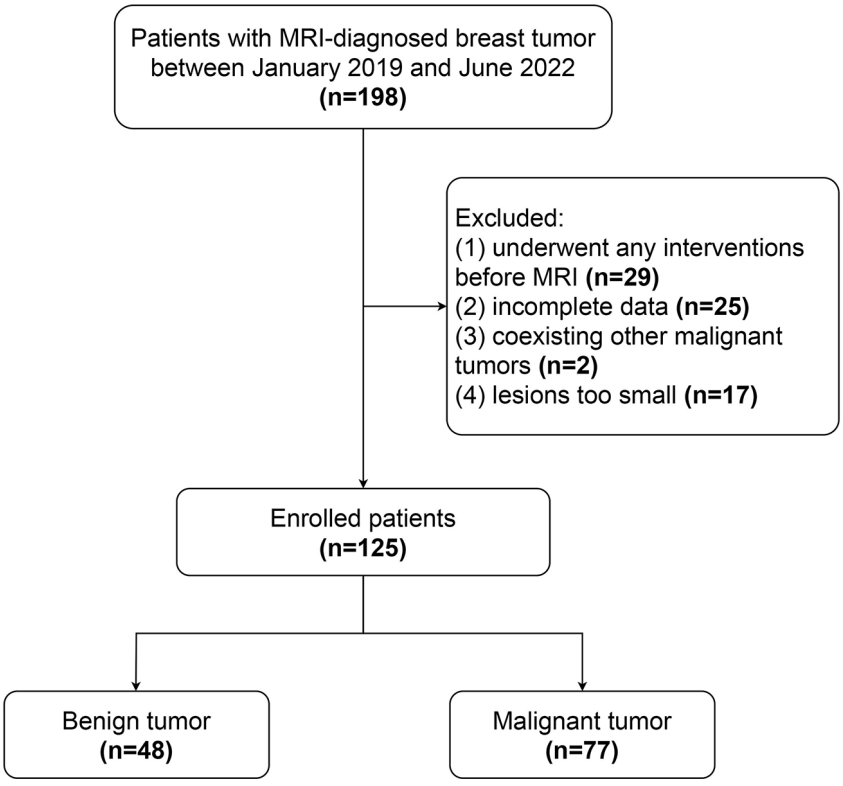

Fig. 1 Flowchart of the patient enrollment process

Table 1 MRI scanning parameters

Parameter	T1WI	T2WI-SPAIR	DWI*	DCE-T1WI
TE (ms)	8	100	85	2
TR (ms)	467	4598	8198	4
Slice thickness (mm)	3.5	3.5	3.5	2
FOV (mm × mm)	250 × 330	250 × 330	250 × 330	250 × 330
Matrix	252 × 261	208 × 261	–	–

*The b-value is 1000 s/mm^2; TE, echo time; TR, repetition time; FOV, field of view

patients. Images were imported into the Philips post-processing workstation for ADC map generation. Utilizing lesion locations from the T2WI-SPAIR and DCE-T1WI, areas with high DWI signal and low ADC signal were marked as the region of interest (ROI), using a b-value of 1000s/mm^2 in the DWI sequence.

Measurements were conducted jointly by two radiologists with over five years of breast diagnostic experience, resolving any disagreements through discussion. The ROI was manually placed on the largest solid area of the lesion, carefully excluding cystic changes, hemorrhage, necrosis, fat, blood vessels, and artifacts. A circular ROI was used for consistency. The ROI was placed to cover the lesion as evenly as possible, ensuring that the entire lesion area was represented. To avoid bias, the ROI placement was done in a blinded manner, with radiologists unaware of the lesion's final pathological diagnosis at the time of image assessment. No specific selection of higher or lower ADC values was made during ROI placement. The minimum and average ADC values (ADC_avg) were measured, along with ADC values from the contralateral pectoralis major muscle, normal glandular tissue, and interventricular septum, which were relatively distant from the lesion and minimally influenced by it. The ROI area ranged from 10–50 mm^2, and measurements were performed on two adjacent slices of the lesion, contralateral pectoralis major muscle, normal glandular tissue, and interventricular septum. For the pectoralis major, the ROI was placed at the center of the muscle to avoid potential signal changes in the peripheral areas. In elderly patients with partial muscle atrophy, the ROI size was proportionally reduced to focus on the preserved muscle fibers. To minimize the impact of cardiac motion artifacts on the measurement of the interventricular septum, the ROI was carefully positioned in the region with the least motion artifact. Additionally, to ensure data accuracy, the physician identified and excluded any outliers during the measurement process, minimizing their impact on the results. An average of three measurements was taken, recording five ADC values for each of the four sites.

The calculation formula was: rADC_min = lesion ADC_min/ADC of the interventricular septum/pectoralis major/glandular tissue (rADC_min_IS, rADC_min_PM, rADC_min_G), obtaining rADC_min values for reference sites and lesion ADC_avg, ADC_min data. Then, the

mean (X) and standard deviation (S) of the three ADC measurements were calculated, and the ADC_cv was determined using the formula CV=S/X. These data were subsequently analyzed. The radiological presentations of breast fibroadenoma and invasive ductal carcinoma are depicted in Fig. 2.

Statistical analysis

Statistical analyses were conducted using R (version 3.6.3) and Python (version 3.7). Continuous variables that followed a normal distribution were described using mean ± standard deviation, and comparisons between groups were performed using the t-test for equal variances (Levene's test $P \geq 0.05$) and Welch's t-test for unequal variances (Levene's test $P < 0.05$). Non-normally distributed variables were described using median values with the 25th and 75th percentiles (M [P25, P75]) and compared using the Mann-Whitney U test. Subsequently, the diagnostic utility of each of the six ADC metrics was evaluated independently using receiver operating characteristic (ROC) curves, which synchronously calculated sensitivity, specificity, Youden's index, and the optimal diagnostic threshold for each variable. Correlation analyses among six ADC metrics were performed using Spearman's method.

Moreover, a combined model incorporating the six ADC metrics and age was developed using a binary logistic regression method with forward and backward stepwise selection based on the Akaike Information Criterion (AIC), and nomogram was generated. The goodness-of-fit, clinical net benefit, and clinical impact of the combined model were assessed using calibration curves, clinical decision curves, and clinical impact curves, respectively. Finally, the comparative analysis of the six ADC metrics and the combined model was performed using the DeLong test, and the improvement in predictive performance for differentiating between benign and malignant breast tumors by the combined model over the optimal single ADC metric was quantified using the integrated discrimination improvement (IDI) index. All statistical tests were two-sided, and $P < 0.05$ was considered statistically significant.

Results

Pathological results

A total of 125 patients diagnosed with breast tumors were included in this study. The cohort consisted of 77 individuals with malignant breast tumors, predominantly invasive ductal carcinoma, with ages ranging from 28 to 77 years (mean age: 55.66 ± 11.21 years). The remaining 48 patients had benign tumors, mostly fibroadenomas, with ages spanning from 10 to 64 years (mean age: 42.96 ± 14.57 years). In the malignant cohort, 65 cases were identified as non-specific invasive carcinoma, 6 as ductal carcinoma in situ, and 1 case each of intraductal papillary carcinoma, lobular carcinoma, neuroendocrine carcinoma, and adenomyoepithelioma. Additionally, 2 cases of other unspecified malignant tumors were included. The benign cohort comprised 35 cases of fibroadenomas, 6 cases of adenosis, 3 cases of inflammatory

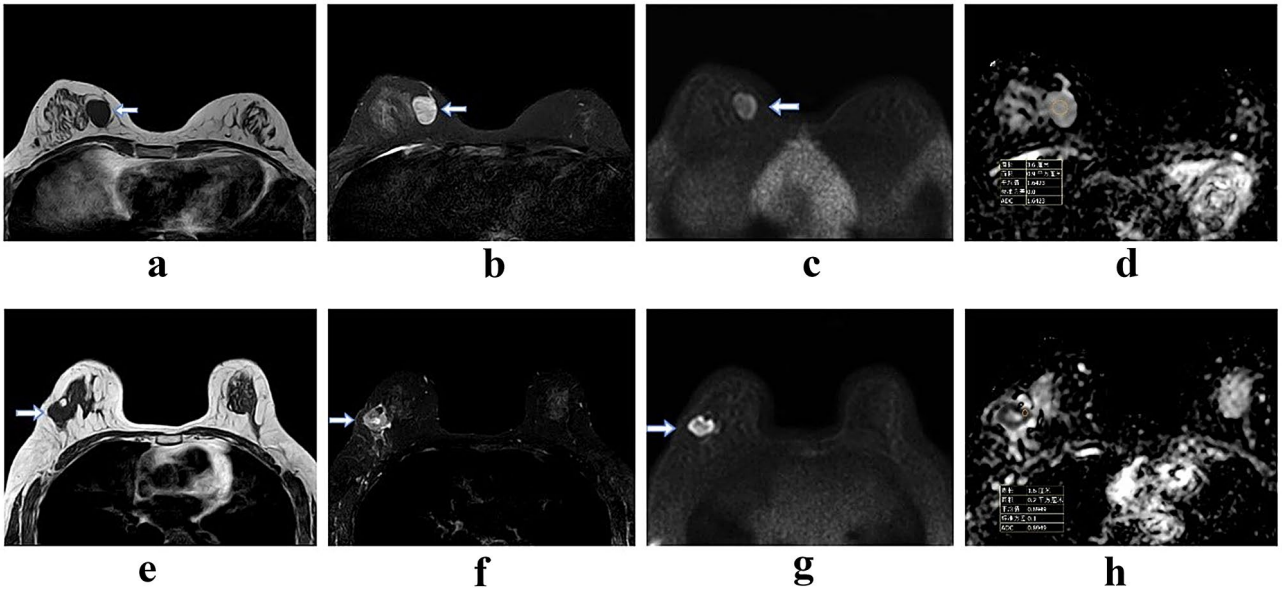

Fig. 2 Comparative MR images of breast lesions in two patients. **a**–**d**: patient with fibroadenoma. **a**: T1WI shows lesion with slightly low signal (arrow); **b**: T2WI-SPAIR shows high signal (arrow); **c**: DWI shows high signal (arrow); **d**: ADC map shows slightly low signal, ADC value at 1.64×10^{-3} mm^2/s (ROI). e–h: patient with invasive ductal carcinoma. **e**: T1WI shows lesion with low signal (arrow); **f**: T2WI-SPAIR shows slightly high signal (arrow); **g**: DWI shows high signal (arrow); **h**: ADC map shows low signal, ADC value at 0.90×10^{-3} mm^2/s (ROI)

Table 2 Comparison of six ADC metrics between benign and malignant breast tumors

Variable (mm^2/s)	Total (n = 125)	Benign group (n = 48)	Malignant group (n = 77)	Statistics	*P*
ADC_avg	0.970 [0.850,1.280]	1.420 [1.200,1.590]	0.880 [0.800,0.960]	8.226	<0.001
ADC_min	0.890 [0.780,1.210]	1.320 [1.110,1.530]	0.800 [0.740,0.900]	8.343	<0.001
ADC_cv	0.080 [0.050,0.130]	0.060 [0.040,0.090]	0.100 [0.070,0.140]	−3.624	<0.001
rADC_min_PM	1.420 [1.000,2.130]	1.970 [1.340,2.540]	1.190 [0.920,1.830]	4.170	<0.001
rADC_min_G	1.108 ± 0.137	1.172 ± 0.108	1.068 ± 0.138	4.677	<0.001
rADC_min_IS	0.640 [0.530,0.870]	0.940 [0.750,1.060]	0.560 [0.490,0.660]	6.906	<0.001

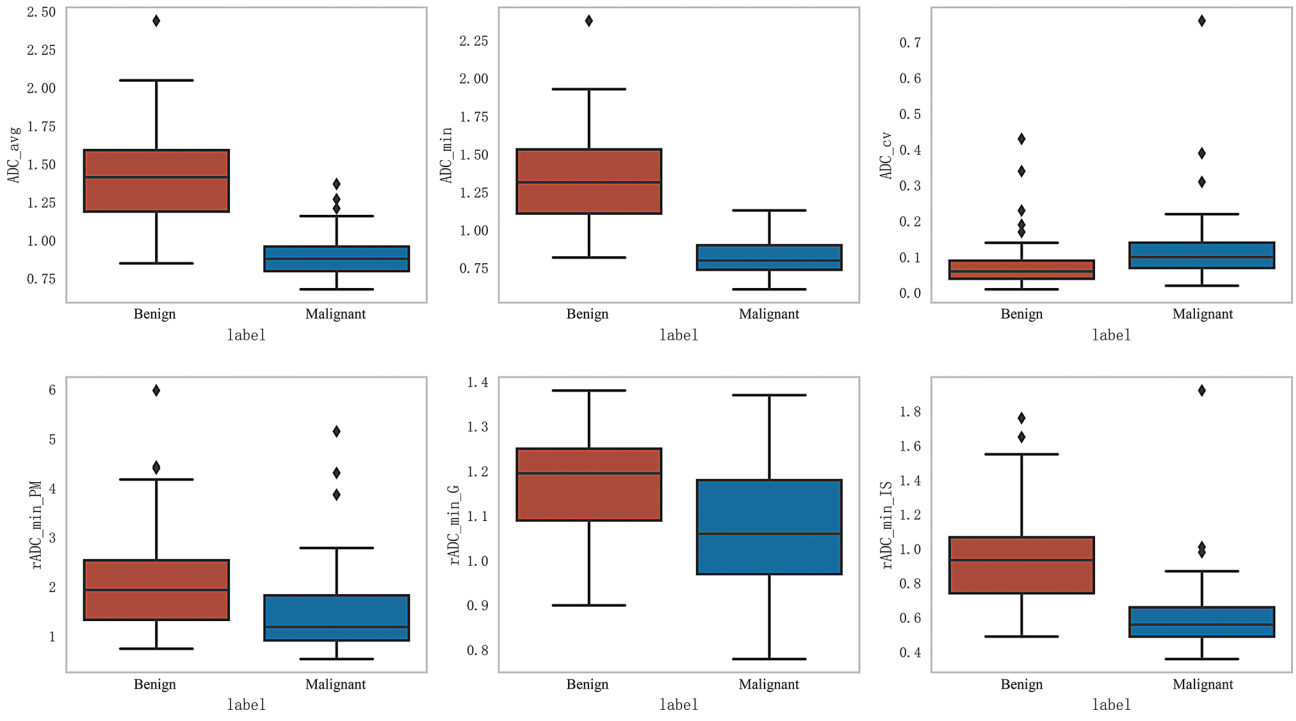

Fig. 3 Box plots of six ADC metrics for benign and malignant breast tumors

changes, 2 intraductal papillomas, 1 case of fibrous hyperplasia, and 1 case of benign phyllodes tumor.

Comparison of six ADC metrics

Statistical analysis revealed significant differences in ADC_avg, ADC_min, ADC_cv and rADC_min values between malignant and benign tumor groups ($P < 0.001$). Specifically, ADC_min, ADC_avg, and rADC_min values were lower in the malignant group compared to the benign group. Conversely, the ADC_cv value was lower in the benign tumor group (Table 2 and Fig. 3). Spearman correlation analysis revealed significant correlations between ADC_min and ADC_avg, as well as between rADC_min_PM and rADC_min_G, respectively. Conversely, ADC_cv displayed a weak negative correlation with all other metrics (Fig. 4).

Diagnostic efficacy of single indicators

In the analysis of diagnostic efficacy of the six ADC metrics for differentiating between benign and malignant breast tumors (Table 3 and Fig. 5), ADC_min exhibited the highest area under the curve (AUC) value, along with superior sensitivity and specificity, whereas ADC_cv demonstrated the poorest diagnostic performance. The AUC values of ADC_avg and ADC_min were closely matched, with no statistically significant difference between them as indicated by the DeLong test (Table 4). Therefore, both metrics may be viable options in clinical diagnosis. Furthermore, among the three relative ADC metrics, rADC_min_IS showed the best diagnostic performance, which could be attributed to the greater stability of the interventricular septum density compared to the other two measures.

Diagnostic efficacy of combined model

In the combined model, only age and ADC_avg were included as feature variables for constructing the nomogram (Fig. 6). The model formula is as follows:

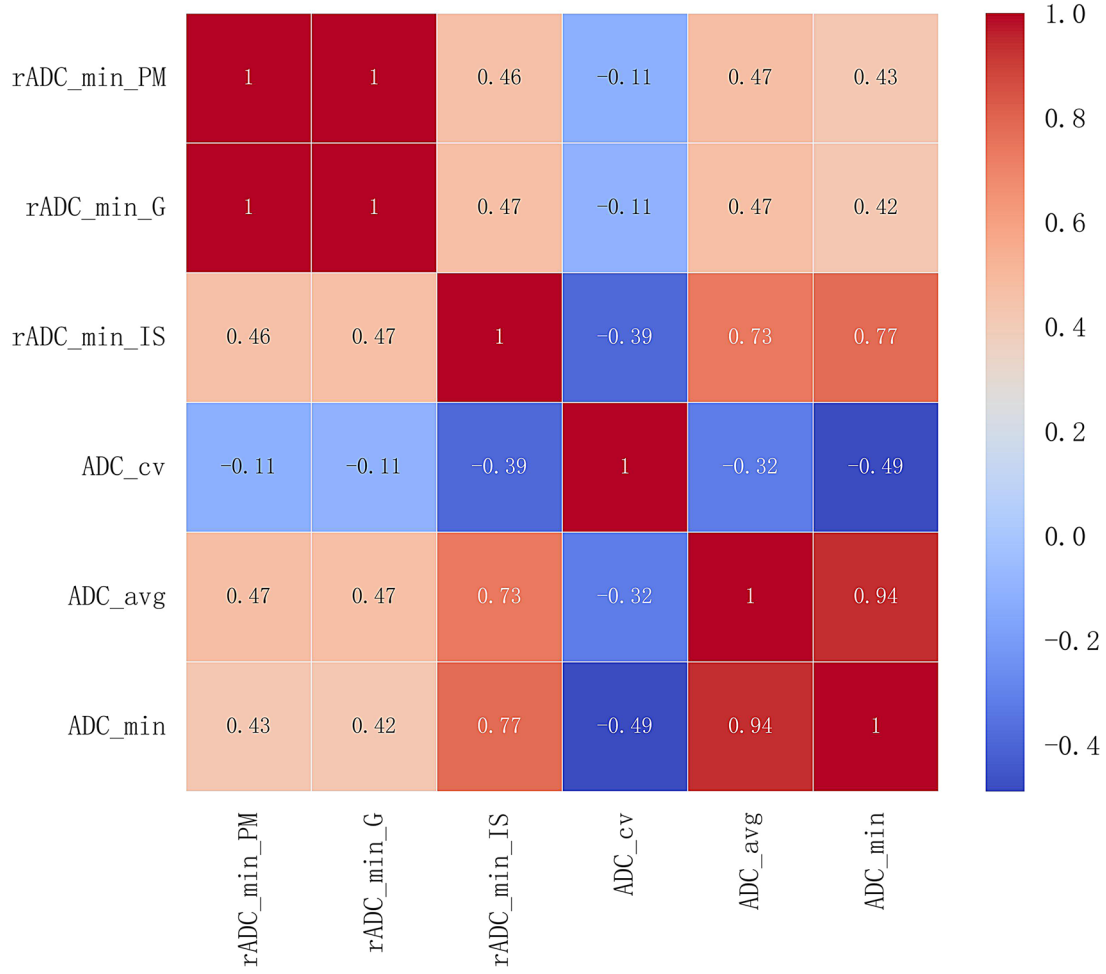

Fig. 4 Correlation analysis heat map of six ADC metrics

Table 3 Results of ROC curve analysis of six ADC metrics and combined model

Variable	AUC	Sensitivity	Specificity	Youden Index	Optimal Threshold
ADC_avg	0.938	0.875	0.857	0.732	1.04
ADC_min	0.945	0.813	0.961	0.774	1.05
ADC_cv	0.693	0.597	0.729	0.327	0.09
rADC_min_PM	0.722	0.833	0.584	0.418	1.28
rADC_min_G	0.721	0.833	0.584	0.418	1.08
rADC_min_IS	0.868	0.75	0.896	0.646	0.75
Combined	0.964	0.987	0.875	0.862	0.376

$$\log\left(\frac{p}{1-p}\right) = 6.061 + 0.126 \times age - 10.832 \times ADC\_avg$$

where p represents the probability of occurrence of malignant breast tumors. The diagnostic performance of the combined model (AUC = 0.964) was superior to that of the individual ADC metrics alone, and the DeLong test revealed statistically significant differences between the diagnostic efficacy of the combined model and all individual ADC metrics. The calibration curve of the combined model showed good agreement with the actual outcomes (Fig. 7), and analyses of clinical decision curves and clinical impact curves also indicated that the nomogram of the combined model achieved a better clinical net benefit (Fig. 8). Finally, the IDI analysis demonstrated that the combined model improved diagnostic performance by 8.3% compared to the optimal single metric (ADC_min), with this result being statistically significant ($P = 0.003$).

Discussion

Breast cancer remains one of the foremost global health challenges. Early and accurate differentiation between benign and malignant lesions is crucial for improving clinical outcomes in breast cancer. DWI and its derived ADC values play a pivotal role in enhancing the diagnostic accuracy of breast MRI. This study contributes to the field by exploring and validating the potential of

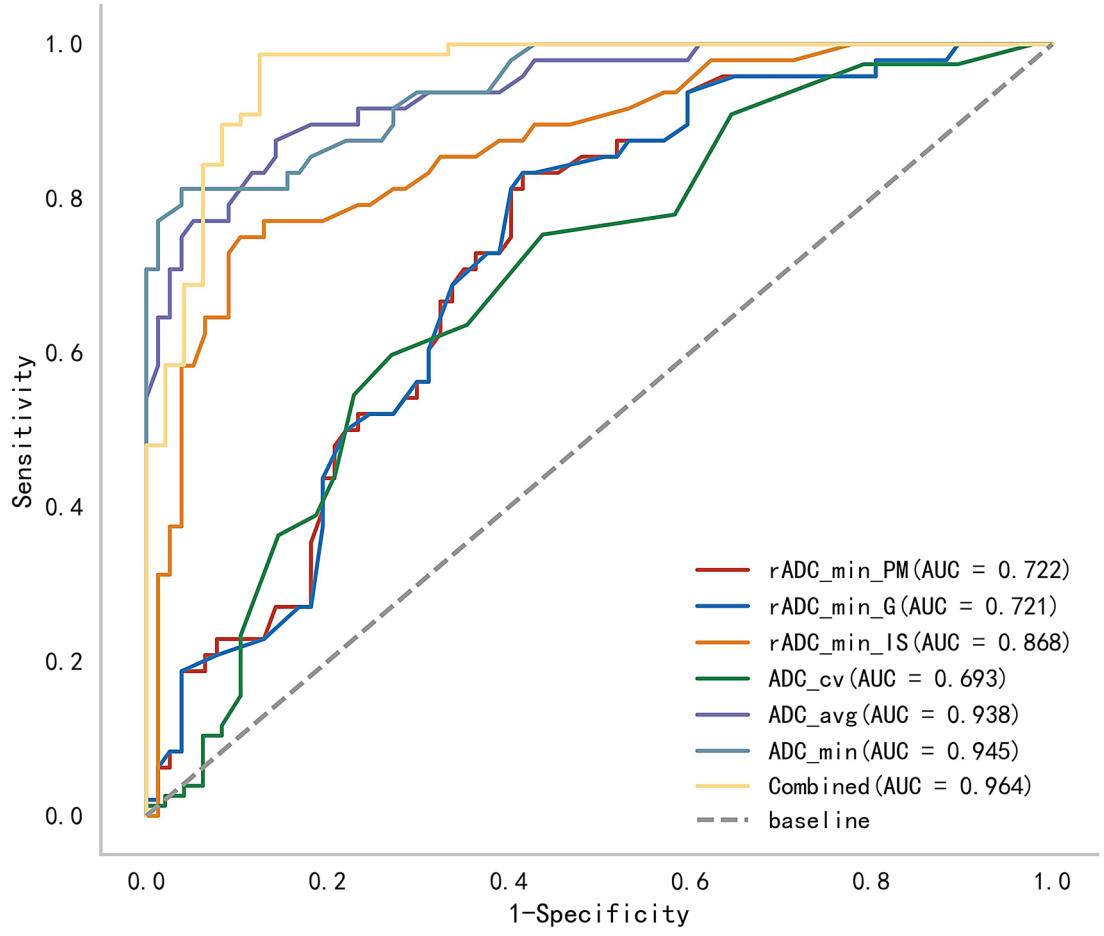

Fig. 5 Roc curves for six ADC metrics and combined model

Table 4 *Z* and *P* values for Delong's test

Variable	rADC_min_PM	rADC_min_G	rADC_min_IS	ADC_cv	ADC_avg	ADC_min
rADC_min_G	$Z=0.582$ $P=0.561$					
rADC_min_IS	$Z=3.118$ $P=0.002$	$Z=3.149$ $P=0.002$				
ADC_cv	$Z=6.015$ $P<0.001$	$Z=5.996$ $P<0.001$	$Z=8.365$ $P<0.001$			
ADC_avg	$Z=4.906$ $P<0.001$	$Z=4.914$ $P<0.001$	$Z=2.524$ $P=0.012$	$Z=11.396$ $P<0.001$		
ADC_min	$Z=5.006$ $P<0.001$	$Z=5.02$ $P<0.001$	$Z=3.125$ $P=0.002$	$Z=10.749$ $P<0.001$	$Z=0.503$ $P=0.615$	
Combined	$Z=13.918$ $P<0.001$	$Z=13.877$ $P<0.001$	$Z=18.573$ $P<0.001$	$Z=5.68$ $P<0.001$	$Z=26.496$ $P<0.001$	$Z=27.451$ $P<0.001$

advanced ADC-derived metrics, including ADC_avg, ADC_min, rADC_min, and ADC_cv, to differentiate benign and malignant breast tumors.

The relationship between ADC values and tumor biology is complex. Numerous studies have highlighted that ADC values are influenced by cellularity, cell membrane integrity, and ECM content [8, 13]. Malignant tumors, with higher cellularity and restricted water diffusion, typically exhibit lower ADC values compared to benign lesions. However, the variability in ADC values across different tumor types and patients underscores the importance of understanding tumor heterogeneity. Despite several meta-analyses on the role of ADC values in assessing breast tumor heterogeneity, contradictions exist between studies. Meyer et al., in their meta-analysis of 28 studies, concluded that ADC values cannot be used to distinguish breast cancer molecular subtypes [14]. In contrast, a meta-analysis by Iima et al., which reviewed 52 studies, indicated that ADC values can serve as molecular biomarkers for estrogen receptor (ER), progesterone receptor (PgR), HER2, and Ki-67 [8]. One reason for this phenomenon may be that previous studies have primarily focused on the diagnostic value of ADC_avg, which may not fully capture tumor heterogeneity [15]. For instance, some breast cancer types, such as mucinous carcinoma, may exhibit higher ADC_avg values despite being malignant, due to their ECM rich in mucin, while certain benign lesions (e.g., abscesses) may show lower

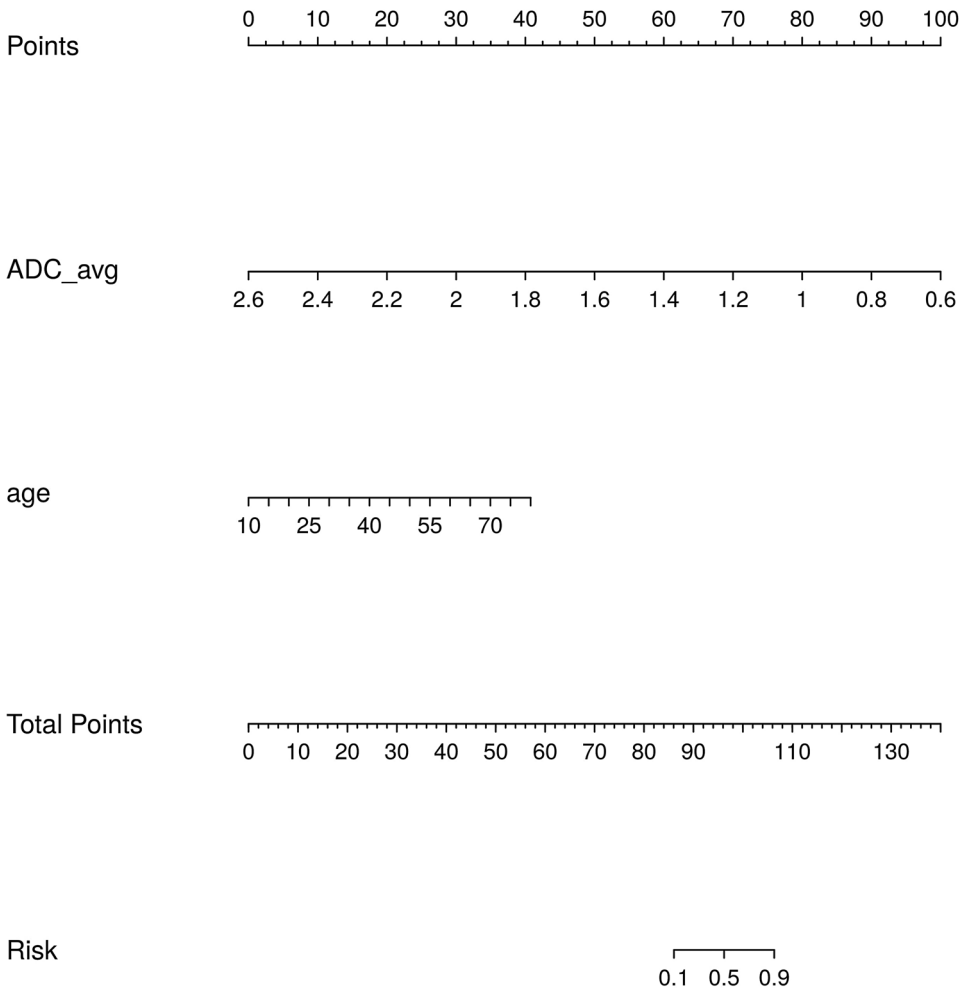

Fig. 6 Nomogram of the combined model

ADC_avg values owing to the presence of necrotic tissue, inflammatory cells, and high-protein exudates that restrict water molecule diffusion [7]. In our study, multiple ADC-derived metrics successfully differentiated benign and malignant breast lesions, not only aligning with existing literature, thus reinforcing the validity of ADC as a characteristic biomarker for breast cancer [16–18], but also providing a more nuanced approach to interpreting ADC.

A meta-analysis by Surov et al., based on 13,847 lesions, proposed an ADC threshold of 1.0×10^{-3} mm²/s as an effective standard for distinguishing benign and malignant breast lesions. This finding is consistent with our study's ADC_avg threshold (1.04×10^{-3} mm²/s) and ADC_min threshold (1.05×10^{-3} mm²/s) [7]. Additionally, in our study, ADC_min, as a single metric, demonstrated optimal performance in distinguishing benign from malignant breast tumors, likely due to its sensitive reflection of the densest, most cell-rich, and diffusion-restricted areas of the tumor, providing critical biological information for diagnosis [19, 20]. Moreover, rADC_min, by normalizing ADC values against reference tissue, improved diagnostic consistency across different patients and scanner types, offering a more standardized approach to tumor characterization [13]. Similarly, quantifying the ADC variability within the tumor using ADC_cv may offer insights into tumor heterogeneity, which is essential for assessing tumor invasiveness and predicting treatment response.

Despite these advantages, individual ADC metrics may still face limitations in clinical applications. Therefore, we explored the potential for constructing a combined predictive model. In constructing this model, we chose ADC_avg over ADC_min, likely because ADC_avg provides a more comprehensive assessment of tumor tissue characteristics, reflecting the average cellular density and tissue integrity across the entire tumor area. This approach accounts for tumor heterogeneity and may provide more consistent diagnostic information across different patients and tumor types. Additionally, the selection of ADC_avg over ADC_min in the combined model also considered its overall performance in

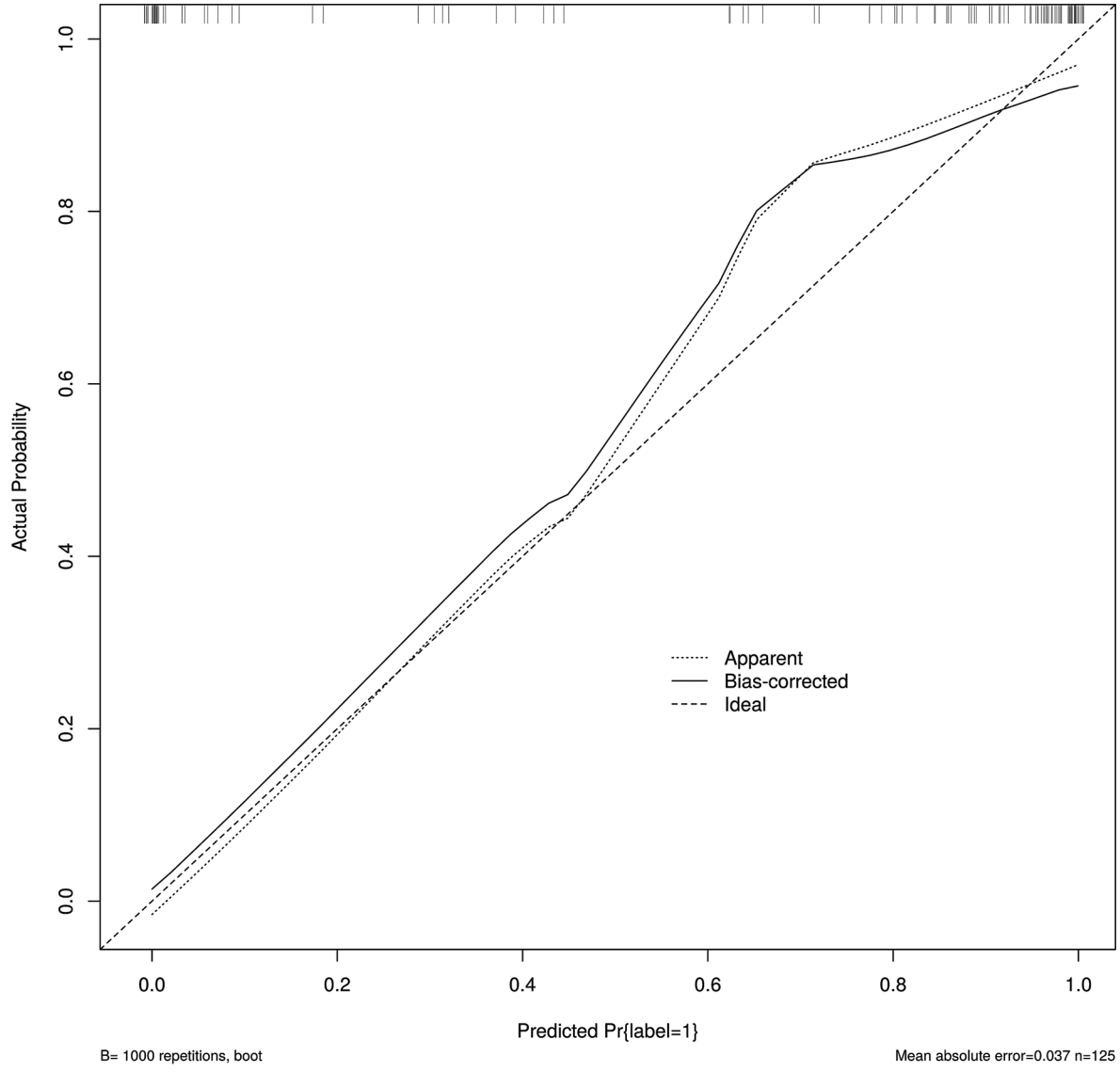

Fig. 7 Calibration curve for combined model

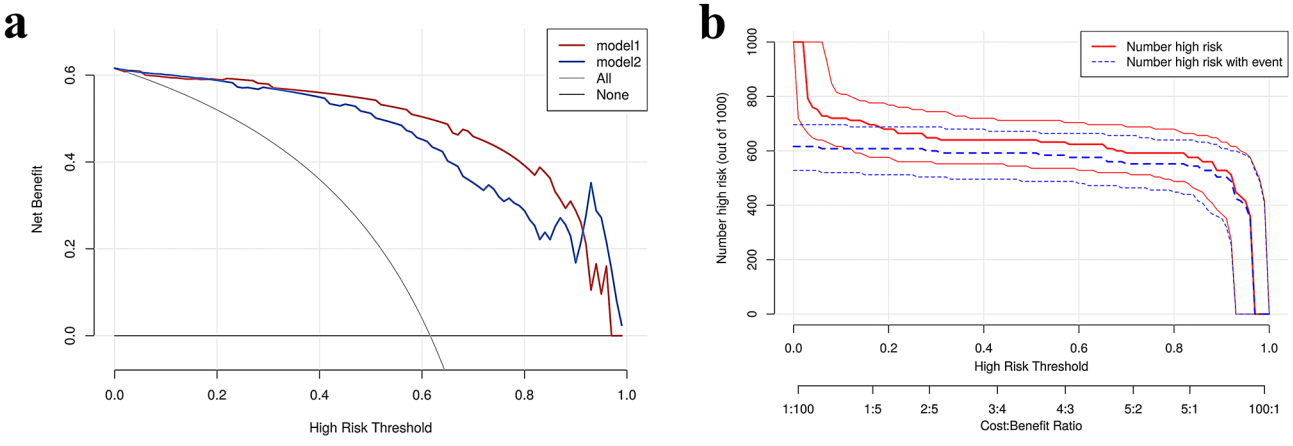

Fig. 8 **a**: Clinical decision curves for the diagnostic efficacy of the combined model (model1) versus ADC_min (model2) for benign and malignant breast tumors; **b**: Clinical impact curve of the combined model

statistical models [21]. When incorporating age, a critical clinical parameter, ADC_avg likely demonstrated better predictive performance due to its representativeness of the overall tumor characteristics. Through the establishment of the combined model, our study further emphasizes the importance of personalized diagnosis, offering a more accurate tool for breast cancer diagnosis.

While our study explored the potential applications of multiple ADC-derived metrics, standardizing their acquisition, processing, and analysis remains a challenge in clinical practice. The placement of ROI during breast DWI analysis is a complex and bias-prone task. Given the inherent heterogeneity of breast tumors, ROI selection may be influenced by various factors such as tumor location, size, and morphological characteristics [22, 23]. In this study, we used circular ROIs to ensure measurement uniformity and avoid areas affected by necrosis, hemorrhage, or cystic lesions. We also utilized multi-point selection to further improve ADC measurement accuracy. Although this method provided consistent results, the ROI placement strategy must be adjusted based on the specific characteristics of each lesion, due to differences in tumor types and histological features. Thus, standardized scanning protocols and ROI placement methods are crucial to ensuring accuracy and reproducibility of results. Future research should explore ways to standardize ROI placement techniques or introduce automated software to reduce human factors, thereby improving DWI reproducibility and clinical applicability [6].

Furthermore, emerging techniques such as DCE imaging, intravoxel incoherent motion (IVIM), and diffusion kurtosis imaging (DKI) may offer additional possibilities for precise imaging diagnosis of breast cancer. A meta-analysis by Zhang et al. suggested that combining DCE with DWI can further enhance the differentiation of benign and malignant breast lesions [24]. IVIM, by separating water diffusion and microvascular perfusion information, provides a more comprehensive characterization of tumor microstructure [25, 26]. DKI can evaluate the non-Gaussian behavior of water molecule diffusion, further enhancing sensitivity to tumor heterogeneity [27]. Although our study did not include DCE, IVIM, or DKI methods, the combination of routine ADC and its derived metrics with age has already shown high predictive performance. We also acknowledge that DWI combined with these emerging techniques may further improve the diagnostic accuracy and early detection capabilities for breast cancer.

Our study highlights the advantages of integrating DWI into routine breast MRI protocols. Firstly, by offering more precise diagnostic methods, it aids physicians in early-stage differentiation of breast tumor nature, facilitating personalized treatment plans for patients. Secondly, the use of these advanced ADC metrics can reduce unnecessary biopsy procedures, minimizing patient discomfort and treatment costs. Lastly, this study underscores the importance of adopting a multiparametric assessment strategy in breast cancer management, which not only enhances diagnostic accuracy but also provides valuable biomarkers for future therapeutic decisions.

Despite providing valuable insights, this study has two limitations. Its retrospective design and single-center sample may introduce inherent selection biases, limiting the generalizability of the results. Future research should employ prospective, multicenter designs to validate our findings. Additionally, the complexity and heterogeneity of breast cancer were only partially addressed, with a lack of in-depth analysis of tumor grading and molecular subtypes. Future studies in these areas may further guide treatment decisions and improve patient outcomes.

Conclusions

This study highlights the value of advanced ADC metrics in differentiating malignant from benign breast lesions. The combination of ADC metrics and patient age improves diagnostic accuracy and offers potential for enhancing clinical decision-making in breast cancer diagnosis.

Abbreviations

ADC	Apparent diffusion coefficient
ADC_avg	Average ADC value
ADC_cv	ADC coefficient of variation
ADC_min	Minimum ADC value
AIC	Akaike information criterion
AUC	Area under the curve
DCE-T1WI	Dynamic contrast-enhanced T1-weighted imaging
DKI	Diffusion kurtosis imaging
DWI	Diffusion-weighted imaging
FOV	Field of view
IDI	Integrated discrimination improvement
IVIM	Intravoxel incoherent motion
MRI	Magnetic resonance imaging
rADC_min	Minimum ratio of ADC
rADC_min_G	Minimum ratio of ADC to the glandular
rADC_min_IS	Minimum ratio of ADC to the interventricular septum
rADC_min_PM	Minimum ratio of ADC to the pectoralis major
ROC	Receiver operating characteristic
ROI	Region of interest
T1WI	T1-weighted imaging
T2WI-SPAIR	T2-weighted imaging with spectral attenuated inversion recovery
TE	Echo time
TR	Repetition time

Acknowledgements

Not applicable.

Author contributions

Conception and design were contributed by JS and YPY. Data acquisition were contributed by YPY. Data analysis and interpretation was contributed by JL. Drafting of the manuscript was contributed by YPY. Critical revision of the manuscript was contributed by JL and JS. All authors read and approved the final manuscript.

Funding
This work was supported by the Medical Research Project of Chengdu Municipal Health Commission of Sichuan Province (Grant Number: 2021428).

Data availability
The datasets used and/or analysed during the current study are available from the corresponding author on reasonable request.

Declarations

Ethics approval and consent to participate
This study was conducted in accordance with the Declaration of Helsinki (as revised in 2013). Ethical approval was granted by the Chongzhou People's Hospital Medical Ethics Committee, and informed consent was waived (Approval No. 2021[5]).

Consent for publication
Not applicable.

Disclosure
In the preparation of this manuscript, the authors utilized the artificial intelligence tool, DeepSeek-R1 (https://chat.deepseek.com/), for language refinement to enhance the readability and clarity of the text. Following the AI-assisted revision, the authors meticulously reviewed and edited the content to ensure accuracy and coherence. The authors take full responsibility for the final content of the manuscript.

Competing interests
The authors declare no competing interests.

Received: 4 April 2024 / Accepted: 28 March 2025
Published online: 11 April 2025

References

1. Tarantino P, Tolaney SM. Progress in breast cancer management. Lancet (London, England). 2024;404(10461):1376–78.
2. Xiong X, Zheng LW, Ding Y, Chen YF, Cai YW, Wang LP, Huang L, Liu CC, Shao ZM, Yu KD. Breast cancer: pathogenesis and treatments. Signal Transduction Targeted Ther. 2025;10(1):49.
3. Kuhl CK, Lehman C, Bedrosian I. Imaging in locoregional management of breast cancer. J Clin Oncol Off J Am Soc Clin Oncol. 2020;38(20):2351–61.
4. Lo Gullo R, Sevilimedu V, Baltzer P, Le Bihan D, Camps-Herrero J, Clauser P, Gilbert FJ, Iima M, Mann RM, Partridge SC, et al. A survey by the European Society of Breast Imaging on the implementation of breast diffusion-weighted imaging in clinical practice. Eur Radiol. 2022;32:6588–97.
5. Dietzel M, Ellmann S, Schulz-Wendtland R, Clauser P, Wenkel E, Uder M, Baltzer PAT. Breast MRI in the era of diffusion weighted imaging: do we still need signal-intensity time curves? Eur Radiol. 2020;30(1):47–56.
6. Boss MA, Malyarenko D, Partridge S, Obuchowski N, Shukla-Dave A, Winfield JM, Fuller CD, Miller K, Mishra V, Ohliger M, et al. The QIBA profile for diffusion-weighted MRI: apparent diffusion coefficient as a quantitative imaging biomarker. Radiology. 2024;313:e233055.
7. Surov A, Meyer HJ, Wienke A. Can apparent diffusion coefficient (ADC) distinguish breast cancer from benign breast findings? A meta-analysis based on 13 847 lesions. BMC Cancer. 2019;19(1):955.
8. Iima M, Honda M, Sigmund EE, Ohno Kishimoto A, Kataoka M, Togashi K. Diffusion MRI of the breast: current status and future directions. J Magn Reson Imaging. 2020;52(1):70–90.
9. Surov A, Clauser P, Chang YW, Li L, Martincich L, Partridge SC, Kim JY, Meyer HJ, Wienke A. Can diffusion-weighted imaging predict tumor grade and expression of Ki-67 in breast cancer? A multicenter analysis. Breast Cancer Res. 2018;20(1):58.
10. Egnell L, Vidić I, Jerome NP, Bofin AM, Bathen TF, Goa PE. Stromal collagen content in breast tumors correlates with in vivo diffusion-weighted imaging: a comparison of multi b-value DWI with histologic specimen from benign and malignant breast lesions. J Magn Reson Imaging. 2020;51(6):1868–78.
11. Li T, Hong Y, Kong D, Li K. Histogram analysis of diffusion kurtosis imaging based on whole-volume images of breast lesions. J Magn Reson Imaging. 2020;51(2):627–34.
12. Tsvetkova S, Doykova K, Vasilska A, Sapunarova K, Doykov D, Andonov V, Uchikov P. Differentiation of benign and malignant breast lesions using ADC values and ADC ratio in breast MRI. Diagnostics (Basel, Switzerland). 2022;12(2):332.
13. Li X, Sun K, Chai W, Zhu H, Yan F. Role of breast MRI in predicting histologic upgrade risks in high-risk breast lesions: a review. Eur J Radiol. 2021;142:109855.
14. Meyer HJ, Wienke A, Surov A. Diffusion-weighted imaging of different breast cancer molecular subtypes: a systematic review and meta-analysis. Breast Care (Basel, Switzerland). 2022;17(1):47–54.
15. Geng X, Zhang D, Suo S, Chen J, Cheng F, Zhang K, Zhang Q, Li L, Lu Y, Hua J, et al. Using the apparent diffusion coefficient histogram analysis to predict response to neoadjuvant chemotherapy in patients with breast cancer: comparison among three region of interest selection methods. Ann Transl Med. 2022;10:323.
16. Gullo RL, Partridge SC, Shin HJ, Thakur SB, Pinker K. Update on DWI for breast cancer diagnosis and treatment monitoring. AJR. 2024;222(1).
17. Bickel H, Clauser P, Pinker K, Helbich T, Biondic I, Brkljacic B, Dietzel M, Ivanac G, Krug B, Moschetta M, et al. Introduction of a breast apparent diffusion coefficient category system (ADC-B) derived from a large multicenter MRI database. Eur Radiol. 2023;33:5400–10.
18. Zhao J, Guan H, Li M, Gu H, Qin J, Wu X. Significance of the ADC ratio in the differential diagnosis of breast lesions. Acta Radiol (Stockholm, Sweden: 1987). 2016;57(4):422–29.
19. Suo S, Zhang K, Cao M, Suo X, Hua J, Geng X, Chen J, Zhuang Z, Ji X, Lu Q, et al. Characterization of breast masses as benign or malignant at 3.0T MRI with whole-lesion histogram analysis of the apparent diffusion coefficient. J Magn Reson Imaging. 2016;43:894–902.
20. Rupa R, Thushara R, Swathigha S, Athira R, Meena N, Cherian MP. Diffusion weighted imaging in breast cancer - Can it be a noninvasive predictor of nuclear grade? Indian J Radiol Imaging. 2020;30(1):13–19.
21. Lin CX, Tian Y, Li JM, Liao ST, Liu YT, Zhan RG, Du ZL, Yu XR. Diagnostic value of multiple b-value diffusion-weighted imaging in discriminating the malignant from benign breast lesions. BMC Med Imaging. 2023;23(1):10.
22. Iima M, Honda M, Satake H, Kataoka M. Standardization and advancements efforts in breast diffusion-weighted imaging. Jpn J Radiol. 2025;43(3):347–54.
23. Wielema M, Dorrius MD, Pijnappel RM, De Bock GH, Baltzer PAT, Oudkerk M, Sijens PE. Diagnostic performance of breast tumor tissue selection in diffusion weighted imaging: a systematic review and meta-analysis. PLoS One. 2020;15(5):e0232856.
24. Zhang J, Li L, Zhang L, Zhe X, Tang M, Lei X, Zhang X. Meta-analysis of dynamic contrast enhancement and diffusion-weighted MRI for differentiation of benign from malignant non-mass enhancement breast lesions. Front Oncol. 2024;14:1332783.
25. Ma W, Mao J, Wang T, Huang Y, Zhao ZH. Distinguishing between benign and malignant breast lesions using diffusion weighted imaging and intravoxel incoherent motion: a systematic review and meta-analysis. Eur J Radiol. 2021;141:109809.
26. Liang J, Zeng S, Li Z, Kong Y, Meng T, Zhou C, Chen J, Wu Y, He N. Intravoxel incoherent motion diffusion-weighted imaging for quantitative differentiation of breast tumors: a meta-analysis. Front Oncol. 2020;10:585486.
27. Li Z, Li X, Peng C, Dai W, Huang H, Li X, Xie C, Liang J. The diagnostic performance of diffusion kurtosis imaging in the characterization of breast tumors: a meta-analysis. Front Oncol. 2020;10:575272.

Publisher's Note